

## Computational Tabulation of the Spatial Origin of Scoring Secondary Electron Tracks in a Wall-less Tissue Equivalent Proportional Counter under Photon Irradiation

F. Ali<sup>1</sup>, A. J. Waker<sup>1</sup> and E. J. Waller<sup>1</sup>

<sup>1</sup> University of Ontario Institute of Technology, Ontario, Canada  
(E-mail of corresponding author: fawaz.ali@uoit.ca)

### Summary

A Tissue Equivalent Proportional Counter (TEPC) is used for radiation monitoring and metrology. Optimization of the design of these devices can be performed by computational modelling. This paper describes a simulation technique developed to understand and model the response of a wall-less TEPC under photon irradiation.

### 1. Introduction

Tissue Equivalent Proportional Counters (TEPCs) are devices used to measure dose equivalent in low energy mixed radiation fields. A typical TEPC consists of a spherical gas cavity surrounded by a solid wall, both of which are composed of tissue-equivalent material. The gas cavity of the counter seeks to replicate a microscopic tissue volume in which energy deposition by secondary charged particles is measured. However, the fact that a large macroscopic counter replicates a microscopic volume produces *wall effects* which results in secondary charged particles depositing more energy in the gas cavity than they should. The figure below illustrates the *re-entry* wall effect and a *wall-less* counter, a variant TEPC design, which is designed to minimize these effects.

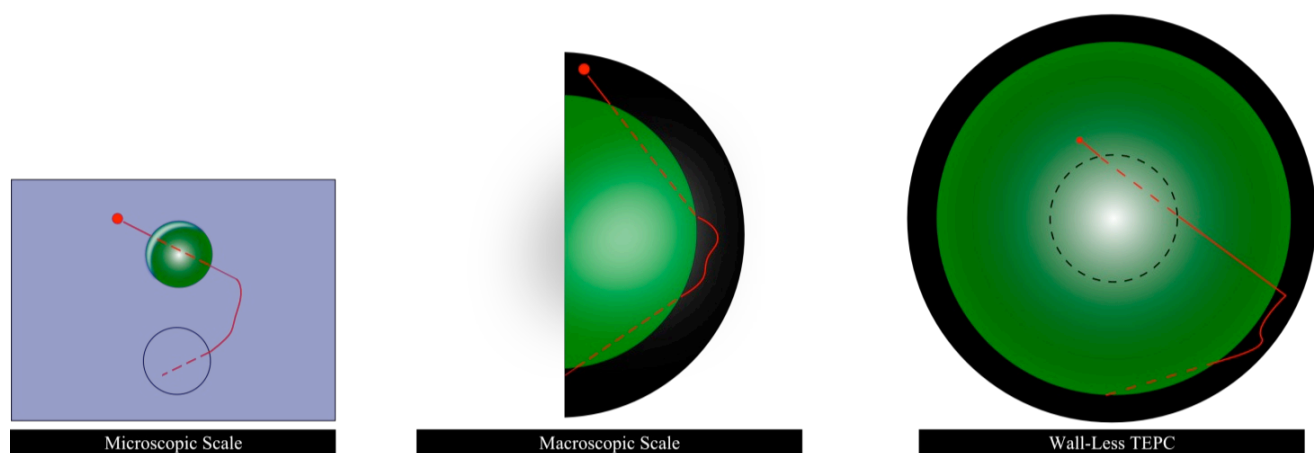


Figure 1 Illustration of Re-Entry Wall Effect and Wall-Less TEPC [1].

For low energy photon fields, the re-entry wall effect is the most important of the three major wall effects. The left-most image in Figure 1 shows that on the microscopic scale, in which the TEPC seeks to replicate energy deposition in, a secondary electron will traverse a volume of interest and will undergo a change in trajectory resulting in it depositing energy in another tissue volume. The difference with the TEPC is that due to the large surface area of its gas cavity, then if the same electron undergoes an identical trajectory on the macroscopic scale, it will traverse the gas cavity twice.

The wall-less TEPC designates a portion of the gas cavity to serve as the sensitive volume of the counter. The third image in Figure 1 shows that this new sensitive volume has a smaller surface area than that of the overall gas cavity thereby better replicating the abovementioned electron's energy deposition in a microscopic volume of tissue. The purpose of this paper is to develop a computational technique to verify if indeed this is the case for a particular wall-less TEPC design irradiated by various monoenergetic photon fields and used to produce bench-mark experimental microdosimetric data.

## 2. Model

The density of gas that fills the sensitive volume of a TEPC is governed by the following equation (in the context of a *spherical* microscopic tissue volume and gas cavity) [2]:

$$\rho_g = \left( \frac{\Delta X_t}{\Delta X_g} \right) \rho_t \quad \text{Where:} \quad (1)$$

$\rho_g =$ gas density (unit: g cm <sup>-3</sup> )	$\rho_t =$ density of tissue (1 g cm <sup>-3</sup> )
$\Delta X_t =$ diameter of tissue volume (unit: μm)	$\Delta X_g =$ diameter of sensitive volume (unit: cm)

Monte Carlo N-Particle eXtended (MCNPX) is a three-dimensional radiation transport code that is used for the investigation carried out in this work. This code will yield information which will be used to quantify the percentage of secondary electrons that deposit energy in the sensitive volume that emanate from various regions of a wall-less TEPC. The scenario modelled in MCNPX replicates the photon irradiation of a wall-less TEPC as performed by Kliauga and Dvorak [3]. The irradiation scenario is illustrated below:

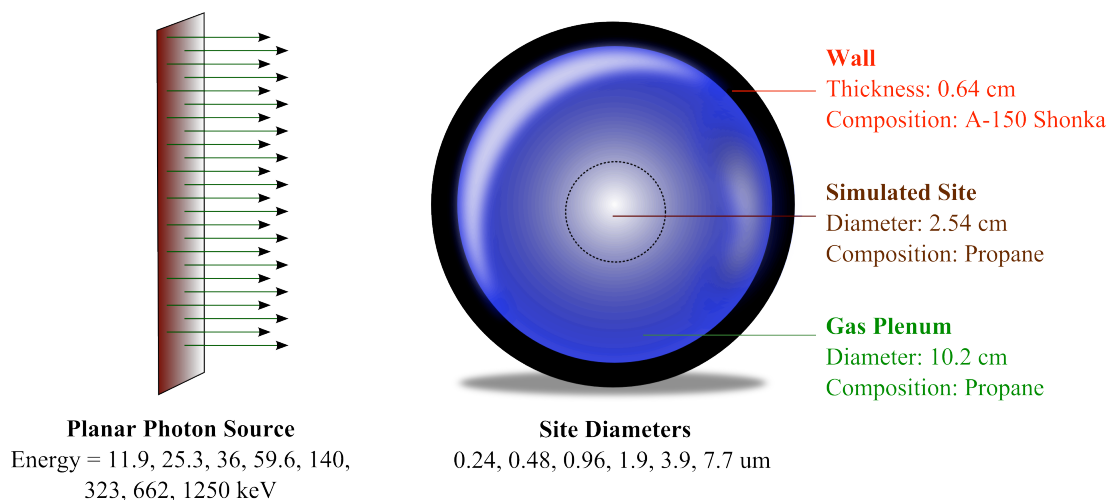


Figure 2 Photon Irradiation of Wall-less TEPC.

Note that the density of gas that fills the sensitive volume, calculated using equation (1), is equal to the gas density that fills the gas plenum that surrounds this sensitive volume. Figure 2 shows that for each of the six microscopic tissue volume diameters, the incident photon energy was successively increased. Thus, a total of 48 MCNPX simulations has been performed whereby each will determine the percentage of the total secondary electrons that traverse the sensitive volume that originate from the wall, gas plenum, and the sensitive volume itself. It is important to note that secondary electron transport must be enabled.

### 3. Method

For every MCNPX simulation, whereby a monoenergetic photon flux of  $10^8$  photons is incident on the wall-less TEPC, the following statement is made in the input file:

```
PTRAC FILE=ASC MAX=2e9 WRITE=ALL EVENT=BNK TYPE=e CELL=1
```

This line instructs MCNPX to print the spatial point of creation of each secondary electron that traverses the sensitive volume (cell 1). This produces a PTRAC file which is a catalogue that contains the aforementioned information for each scoring secondary electron. In the context of a single interacting source photon that produces secondary electrons that in turn traverse the sensitive volume, the contents of this file are described in Figure 3 below.

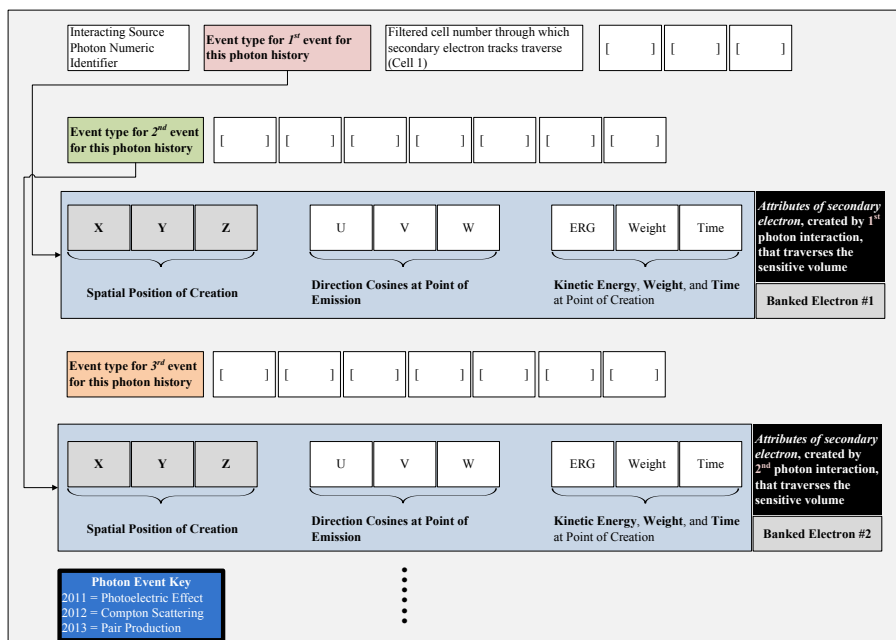


Figure 3 Description of PTRAC File Contents for Scoring Secondary Electrons.

The PTRAC file is fed into a MATLAB M-File which in turn determines which counter region each secondary electron that traverses the sensitive volume was created in. It is important to note that the PTRAC data file size can become quite large (over 500 MB) and in such situations, the file is split into several sub-files using the HJSplit 3.0 software, each of which are then fed into the abovementioned M-File.

#### 4. Results

Figure 4 displays the percentage of the total secondary electrons that traverse the sensitive volume of the wall-less TEPC that originate from the wall and gas plenum as a function of simulated microscopic tissue volume diameter and incident photon energy. Note that the percentage for electron tracks emanating from the sensitive volume itself is omitted as it was consistently found to be on the order of fractions of a per cent.

Several conclusions can be drawn from this figure, the first of which is that the contributions from the wall and gas plenum are independent of the simulated microscopic tissue volume diameter and therefore gas density. Secondly, as the incident photon energy increases, the percentage of scoring electron tracks that emanate from the wall decrease while that from the gas plenum increases. Using a first principles approach, this can be understood since the higher the energy of a photon, the lower the linear attenuation coefficient will be for its wall traversal thereby increasing its chance of penetration which in turn enables it to deposit some of its energy in the gas plenum by ionizing orbital electrons that can go on to traverse the sensitive volume. Lastly, for all incident photon

energies, the number of secondary electrons that emanate from the wall is significantly larger than those from the gas plenum. Relative to the gas plenum, the higher density of the solid wall results in photons having larger linear attenuation coefficients thereby resulting in more secondary electrons being produced within it.

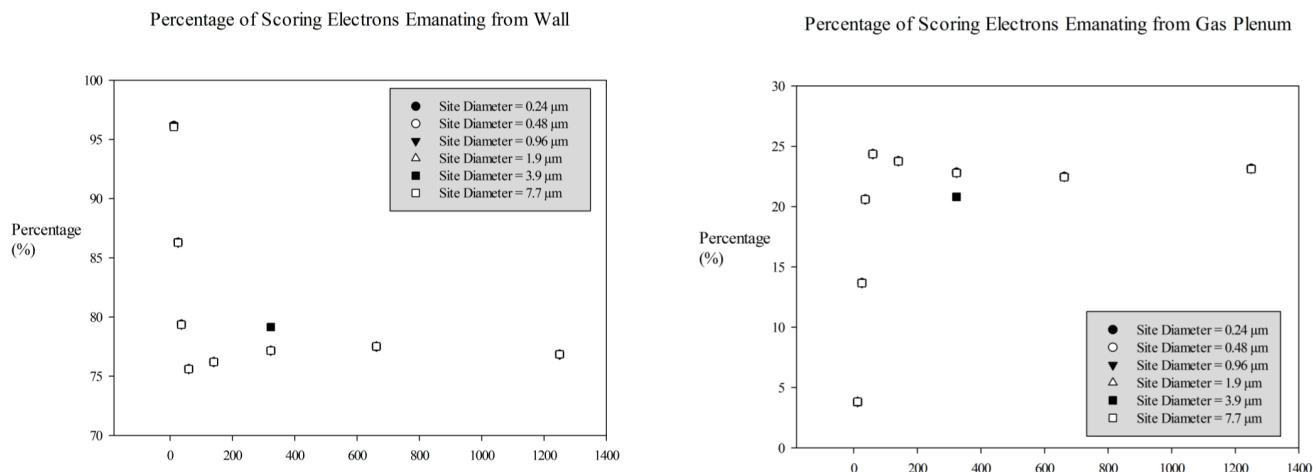


Figure 4 Percentage of Scoring Electrons from Wall and Gas Plenum.

## 5. Conclusion

A computational approach, using MCNPX, to determine the spatial origin of secondary electrons that traverse the sensitive volume of a wall-less TEPC has been presented. It was found that for all incident photon energies, the contribution from the wall is far greater than that from the gas plenum. This simulation framework will be extended to quantify the ability of the wall-less counter to minimize the re-entry wall effect for the monoenergetic photon fields of interest in this study and to assist us in the design of a wall-less counter system suitable for determining the microdosimetric properties of low energy photons and beta rays.

## 6. References

- [1] Kellerer, A. M., "Event Simultaneity in Cavities: Theory of the Distortions of Energy Deposition in Proportional Counters", *Radiation Research*, 48, 2, 1971, 216-233.
- [2] Waker, A. J., "Principles of Experimental Microdosimetry", *Radiation Protection Dosimetry*, 61, 4, 1995, 297-308.
- [3] Kliauga, P., and Dvorak, R., "Microdosimetric Measurements of Ionization by Monoenergetic Photons", *Radiation Research Society*, 73, 1, 1978, 1-20.